AIAA JOURNAL
Vol. 38, No. 4, April 2000

Large-Eddy Simulations: Where Are We and What Can We Expect?

Javier Jiménez*
Universidad Politécnica de Madrid, 28040 Madrid, Spain
and
Robert D. Moser†
University of Illinois at Urbana–Champaign, Urbana, Illinois 61801

Recent subgrid models for large-eddy simulations of turbulent flows are evaluated, particularly the dynamic-Smagorinsky combination, with emphasis on identifying the reasons for their success and the limits of their applicability. The argument is made that they reproduce the turbulent dissipation relatively well, but their main advantage is that they are robust to errors in that they have a built-in mechanism to adjust the dissipation without substantially modifying the larger scales. The question of the stresses is considered next. It is found that it is an intrinsic property of subgrid models that the stresses are essentially unpredictable, and the models considered are indeed found not to reproduce them correctly, even on the average. In particular, the stress-strain correlation is low in real turbulence, and because eddy viscosity models assume that both are proportional, they always result in either the wrong energy spectrum or the wrong stresses. This is confirmed by simulations of shear flows, where it is shown that the error of the mean flow can only be made small if the subgrid stresses are negligible. Stresses are however large-scale quantities that are carried by the resolved scales if the resolution is fine enough. Explicit limits are given.

I. Introduction

LARGE-EDDY simulations (LES) have been shown in the past decade to predict remarkably well the mean properties of turbulent flows of moderate complication. Recent reviews can be found in Refs. 1–5 and will not be repeated here. Dynamic models were introduced in Ref. 6 after earlier related work in Ref. 7 and have proved especially successful. Much of the modern work in the reviews just cited is loosely based on the dynamic idea. Their theoretical basis and practical applications are summarized in Refs. 8 and 9. Some of the reasons for their success are well understood. Their behavior as the flow becomes smooth, such as near walls or during transition, is better than that of other hand-tuned models. Because they are constructed to generate an effective viscosity that is proportional to some measure of the turbulent energy at the small-scale end of the spectrum, their eddy viscosity vanishes as the flow becomes laminar. This alone would justify their use over that of simpler models.

But beyond this obvious advantage, which is confined to inhomogeneous and evolving flows, the reason why they also work better in simpler homogeneous, or fully turbulent, cases, and of how they do it without any obvious adjustable parameter, is not clear. It is also surprising that they, together with other models, work well in shear flows, even though it has been known for a long time that the correlation between the predicted and the true subgrid stresses is very poor.[7,10] Further, it is not known whether this poor prediction of subgrid stresses can be improved upon, or what is required of a subgrid model for an LES to predict the statistical quantities of interest. This lack of understanding of a useful tool is disturbing, not only as an intellectual challenge, but because it raises doubts as to whether it will work in new situations.

In this paper we attempt to clarify these questions: why and how subgrid models based on an eddy viscosity work. This will give us a better idea of the situations in which they can be expected to be useful and of what is needed to improve them. It will also provide us with explicit estimates of the resolution that they require. Isotropic flows are treated first, including limits on the veracity of LES models. This is followed by shear flows and by general conclusions.

Received 2 June 1998; presented as Paper 98-2891 at the AIAA 29th Fluid Dynamics Conference, Albuquerque, NM, 15–18 June 1998; revision received 30 July 1999; accepted for publication 8 August 1999.

*Professor, School of Aeronautics, Plaza Cardenal Cisneros 3; currently Senior Fellow, Center for Turbulence Research, Stanford University, Stanford, CA 94305-3030.

†Professor, Department of Theoretical and Applied Mechanics, 104 South Wright Street.

II. Isotropic Turbulence

A. Numerical Experiments

We will restrict ourselves in this section to temporal isotropic decay, as a model for grid-generated turbulence,[11] and we will discuss a series of experiments[12] intended to clarify the behavior of the simplest formulation of the dynamic model.[13] We establish the notation first.

Consider two filters with characteristic widths δ and $\Delta = 2\delta$. In all of our experiments, the filters are spectrally sharp, the code is spectral on a triply periodic cubic box[14] with 32^3 Fourier modes before dealiasing, and the narrower filter coincides with the grid.

The initial conditions are obtained by filtering a higher resolution flowfield, which had been left to decay to an energy and spectrum closely resembling those at their first experimental section in Ref. 11. Because the field is disturbed by the initial filtering operation, it takes a few time steps for the cascade to recover, but the decay is approximately self-similar after that.

For the grid- and test-filtered velocity fields we compute Reynolds stresses and rate-of-strain tensors that we will call τ_{ij}, σ_{ij}, and T_{ij}, S_{ij}, respectively. The test-filtering operation will be denoted by $[\cdot]$, whereas an overbar will be reserved for averaging over the whole flowfield. Because of our choice of the narrow filter, there is no explicit grid-filtering operation, although our numerical results should be compared to experiments filtered at width δ.

Inner products and norms are defined as L_2, so that $|\boldsymbol{S}|^2 = S_{ij}S_{ij}$. Bold-faced variables will be used from now on for vector or tensor quantities, whereas the same variables in regular typescript represent norms. We introduce the Smagorinsky weighted strains

$$\boldsymbol{M} = 2\sqrt{2}\Delta^2|\boldsymbol{S}|\boldsymbol{S}, \qquad \boldsymbol{m} = 2\sqrt{2}\delta^2|\boldsymbol{\sigma}|\boldsymbol{\sigma} \tag{1}$$

and the differences

$$\boldsymbol{L} = \boldsymbol{T} - [\boldsymbol{\tau}], \qquad \boldsymbol{g} = \boldsymbol{M} - [\boldsymbol{m}] \tag{2}$$

The Smagorinsky assumption at both filter levels is that

$$\boldsymbol{T}^* + c\boldsymbol{M} = 0, \qquad \boldsymbol{\tau}^* + c\boldsymbol{m} = 0 \tag{3}$$

leading to the tensor equation

$$\boldsymbol{\lambda} \equiv \boldsymbol{L}^* + c\boldsymbol{g} = 0 \tag{4}$$

where $\boldsymbol{L}^* = \boldsymbol{L} - \frac{1}{3}\,\mathrm{tr}(\boldsymbol{L})\boldsymbol{I}$ is the traceless projection. This equation is solved for c by contracting Eq. (4) with the tensor $\boldsymbol{g}$, which minimizes the L_2 norm of the residual.[13] When this is done locally, numerical instabilities arise because of artificially high backscatter at those points at which c becomes negative, and this is cured by averaging c over the whole flowfield:

$$c = -f\frac{\overline{\boldsymbol{L}^* \cdot \boldsymbol{g}}}{\overline{|\boldsymbol{g}|^2}}, \qquad f = 1 \tag{5}$$

where the unit factor f is introduced for later convenience. Other strategies have been proposed, and in particular the original formulation of the model used $\boldsymbol{S}$ as the contracting tensor.[6] We will not discuss that formulation here, but other experiments indicate that its performance is similar to Eq. (5).

The final step of the model is to apply Eq. (3) for the calculation of $\boldsymbol{\tau}$ in the equations of motion.

B. Robustness

To understand the response of Eq. (5) to artificial perturbations, a series of numerical experiments was undertaken in Ref. 12 in which errors were purposefully introduced by changing the arbitrary factor f.

As expected, the initial rates of decay were changed proportionally to the change of f, but, somewhat surprisingly, the effect was only temporary and the logarithmic rate of decay soon recovered to a value very close to the undisturbed case and to the experiments. The only lasting effect of the prefactor was an offset in the initial conditions (upper set of curves in Fig. 1).

The reason for this is clear once the spectra of the decaying turbulence are examined (Fig. 2). The spectrum computed with $f = 0.5$ has too much energy in the small scales, whereas the one computed with $f = 2$ is damped in that region. The large scales, on the other hand, are very similar in the three cases, even if the total energy in the flow has decayed from the initial condition by more than a factor of two. The energy differences seen in Fig. 1 are almost totally caused by the differences in the high wave numbers of the spectra, whereas the large scales are unaffected by the change of the subgrid model.

In fact, if the energy of the flow is measured by filtering at the test level, which could be argued to be a more natural measure of performance, the three runs are indistinguishable (lower set of curves in Fig. 1), although they are separated by a factor of four in the definition of the model.

This is consistent with the classical idea that the rate of energy decay is fixed by the large scales of the flow (the production), whereas

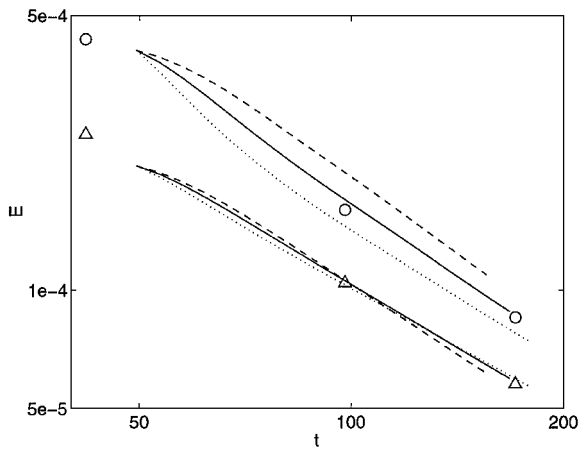

Fig. 1 Decay of filtered energy for modified dynamic models: ○ and upper set of lines, filtered at grid level; △ and lower lines, filtered at test level; ——, $f = 1$; – – –, $f = 0.5$; and · · · · , $f = 2$. Symbols are experiments in Ref. 11.

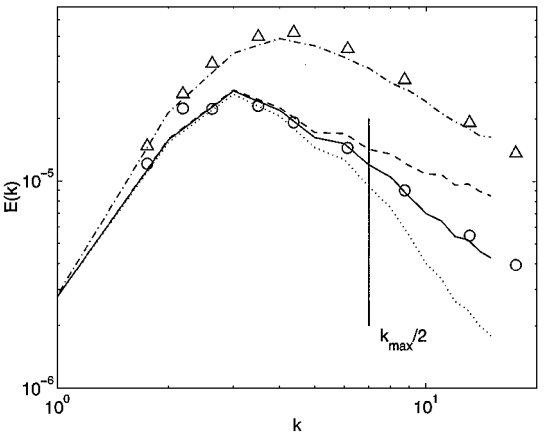

Fig. 2 Energy spectra of modified dynamic LES runs: – · –, initial numerical spectrum at $t = 42$; and △, experimental data at the same time[11]; all other symbols as in Fig. 1 at $t \approx 98$.

the small scales adjust themselves to dissipate whatever energy is fed to them by the cascade.

The way in which the adjustment occurs in this particular case is also clear. Consider first the classical Smagorinsky model in which c is a predetermined constant. The dissipation of the model is then $\boldsymbol{\tau}\cdot\boldsymbol{\sigma} \sim c|\boldsymbol{\sigma}|^3$. If c is chosen too low, not enough energy is dissipated at the small scales to absorb the flux cascading from the larger ones, and energy accumulates in the high wave numbers. This in turn raises $|\boldsymbol{\sigma}|$ and increases the dissipation, until both rates are again in equilibrium. Because, for a $k^{-5/3}$ spectrum, the strain depends mainly on the high wave numbers, which contain little energy, the adjustment can be accomplished with relatively little effect on the total energy of the flow, and the model is robust to mistuning of the constant c. The Smagorinsky model is in this sense slightly superior to regular viscosity because it makes the dissipation proportional to the cube of $|\boldsymbol{\sigma}|$, rather than to the square, and is therefore able to adjust itself with milder effects on the total energy.

If, in addition, we accept the last octave of the spectrum as a sacrificial range of scales, available as a buffer for the model, the effect of the errors in c is minimal, as is the case for the lower set of lines in Fig. 1.

Robust subgrid models should, from this point of view, contain a sensor of the state of the small scales, which in the present case is $|\boldsymbol{\sigma}|$, and a feedback actuator to counter the deviation of the results of the sensor from some local equilibrium. In the models analyzed in this paper, the actuator is almost invariably an eddy viscosity with an adjustable coefficient. The robustness of the model to inaccuracies of its physical assumptions is equivalent to the efficiency of this feedback loop.

C. Hyper-Smagorinsky Models

This analysis suggests that subgrid models could be made more robust than Smagorinsky by making their dissipation dependent on measures that are more concentrated toward the high-wave-number end of the spectrum, in such a way that they can be adjusted with even smaller effects on the total energy.

This was illustrated in Ref. 12 by considering a family of hyper-Smagorinsky models:

$$\boldsymbol{\tau}^* = -c_n|\boldsymbol{\sigma}_n|\boldsymbol{\sigma}, \qquad |\boldsymbol{\sigma}_n|^2 = \int k^{2n}E(k)\,\mathrm{d}k \tag{6}$$

The case $n = 1$ is a global Smagorinsky scheme, in which $|\boldsymbol{\sigma}|$ is computed over the whole field rather than locally. Because of the higher powers of k inside the integral (6), the hyper-strain $\boldsymbol{\sigma}_n$ depends more locally on the tail of the spectrum when $n > 1$, and the models should be able to adjust the dissipation on the basis of information local to the high-wave-number end of the spectrum before it affects the total energy. This is confirmed by Fig. 3, where the prefactor technique is applied to several hyper-Smagorinsky models. For each value of n, the optimal constant c_n was determined empirically to make the energy decay approximately as in the experiment

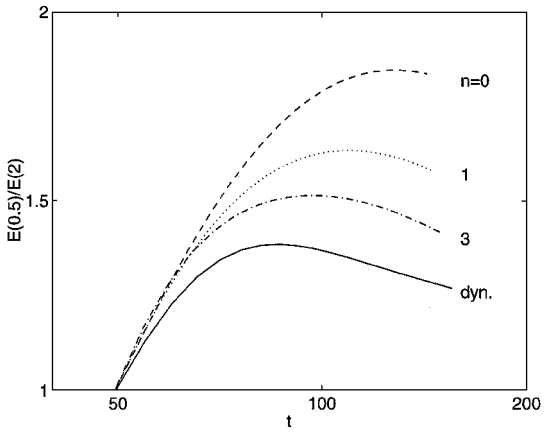

Fig. 3 Ratio of energy obtained for different hyper-Smagorinsky models with $f = 0.5$ and 2: ——, dynamic model; – – –, $n = 0$; · · ·, $n = 1$; and – ·–, $n = 3$.

and the constant was then modified by using fc_n, with $f = 0.5$ and 2, instead of c_n. The ratio between the energies obtained using the two prefactors is a measure of the sensitivity of the model to errors and would be unity for an ideal scheme.

Figure 3 clearly shows that the hyper-Smagorinsky models approach the ideal behavior as n increases, but they never reach it because they use an eddy viscosity, which cannot change the total dissipation without affecting broad ranges of the spectrum. A still better family of models would have a hyperviscosity component, but such models are numerically inconvenient and are not explored here. The dynamic model is also included in Fig. 3 and is shown to behave best of all, with a sensitivity that is roughly half that of Smagorinsky. This is easy to understand because the effect of large n is to concentrate the model feedback sensor near the end of the spectrum, and the dynamic model uses exclusively information from the last octave to compute its constant through the effect of the two filters. It should therefore be nearly optimal among eddy viscosity models with respect to robustness.

In all of these cases, the initial jump of the energy ratio corresponds to a transient in which the spectrum adjusts itself to the incorrect dissipation and accumulates or loses energy at the small scales.

D. Why Does the Dynamic Model Work Better?

We have just shown one of the reasons why a dynamic model would work reasonably well, even if its formulation were considerably in error with respect to the true dynamics of turbulence. However, a simple inspection of the spectra in Fig. 2 shows that the standard formulation (5), with $f = 1$, is very close to the truth because the tail of its spectrum matches the experimental measurements much better than any of the modified models.

The classical explanations for this good performance are, first, that the two Smagorinsky assumptions in Eq. (3) enforce a scale similarity between the two filter levels, which mimics the scale invariance in the inertial range[6] and, second, that the least-squares approximation of Eqs. (4) and (5) ensures that the original Smagorinsky assumptions are reasonably well satisfied.[13]

Both explanations are unlikely. In the first place the Reynolds numbers in the experiment[11] are fairly low ($Re_\lambda \approx 60$), and the spectra do not contain an inertial range. Their slopes are close to $k^{-4/3}$, and obtaining a $k^{-5/3}$ inertial range requires choosing a prefactor $f \approx 1.5$.

Next, the original stress-similarity argument requires that the constant c obtained from Eq. (5) satisfies the tensor equation (4) in some approximate way. But an approximation can be optimum and still be a very bad model for the data. This is unfortunately the case in Eq. (4). A good approximation would require that $|\boldsymbol{\lambda}|^2/|\boldsymbol{L}^*|^2 \ll 1$, which in turn would imply a high correlation between the tensors $-c\boldsymbol{g}$ and $\boldsymbol{L}^*$. This can be tested from the results of the calculation, and Ref. 12 shows that the correlation coefficient

$$\gamma = -\frac{\overline{\boldsymbol{L}^* \cdot \boldsymbol{g}}}{(\overline{|\boldsymbol{g}|^2}\,\overline{|\boldsymbol{L}^*|^2})^{\frac{1}{2}}} \tag{7}$$

after an initial transient, saturates around 20%. Because $\overline{|\boldsymbol{\lambda}|^2}/\overline{|\boldsymbol{L}^*|^2} = 1 - \gamma^2$, this implies that 95% of the magnitude of the stresses remain unexplained by their dynamic Smagorinsky approximation, as already noted in Ref. 7 for simpler Smagorinsky models.

The correlation just quoted is in fact high because it is easy to estimate that, for isotropic turbulence in the inertial range and under fairly mild approximations, the correlation between the subgrid stress and the strain tensor at the same filter width is of the order of 20–30% (see Appendix). Because the subgrid stress decreases with the filter width while the strain increases, $\boldsymbol{L}$ is essentially the stress at the test level, whereas $\boldsymbol{g}$ is essentially the strain at the grid level. The correlation in Eq. (7) therefore tests tensors whose scales are separated by a factor Δ/δ and should in principle be expected to be smaller than that between tensors at the same width. That an LES flow shows higher correlations than a natural one is probably because the former is being driven at the smallest scales by stresses which are, by design, fully correlated with the strains.

Note that the poor correlation of the stress and strain tensors is related to energy backscatter. It is, for example, easy to show that, if τ and S were scalar variables with a joint-normal distribution and with correlation coefficient γ, the fraction of points with negative energy dissipation $\tau S < 0$ would be

$$\tfrac{1}{2} - \sin^{-1}(\gamma)/\pi \tag{8}$$

For $\gamma \approx 0.2$ this amounts to approximately 40% of the points, which is in rough agreement with observed values.[15]

These results show that the Leonard stress $\boldsymbol{L}^*$ and the Germano strain $\boldsymbol{g}$ are far from being coaxial and that any attempt to model one as proportional to the other is doomed to failure. On the other hand, the fact that the method works proves that something is being modelled. Bardina et al.[7] noted that the correlation between the model and flow dissipations was much higher than that for the stresses, and one can easily see that Eq. (5) is actually a dissipation formula. The least-square approximation results in an exact cancellation of the projection of the tensor over one of its summands, and the projection of the stress on the strain is the dissipation. In fact Eq. (5) can be rewritten as

$$\boldsymbol{\tau}_g = -c\boldsymbol{g}, \qquad \overline{\boldsymbol{L}^* \cdot \boldsymbol{g}} = \overline{\boldsymbol{\tau}_g \cdot \boldsymbol{g}} \tag{9}$$

which says that the dissipation generated by the Smagorinsky stresses $\boldsymbol{\tau}_g$ is the same as the production of the Leonard stresses. Because $\boldsymbol{L} = \boldsymbol{T}$ in any numerical flow without an explicit grid filter, the Leonard production can be used as a surrogate for the production at the test level.

Although this argument is suggestive, it is difficult to go much further. Direct computation shows that none of the actual productions and dissipations really match in the dynamic approximation. The numerical production $-\boldsymbol{T} \cdot \boldsymbol{S}$ remains about two times smaller than the dissipation of the Smagorinsky stresses, mainly because a substantial amount of energy is dissipated by the subgrid model on the flow scales between the test and grid filters. Other combinations can be tested with a similar lack of success. Although there is qualitative agreement in all of the obvious balances, the quantitative details are always masked by the broad support of the second-order dissipation. Equation (9), while indicative, does not correspond directly to any physical property of the flow.

III. Predictability of the Subgrid Stress

In the preceding experiments we showed that eddy viscosity models, such as Smagorinsky and the dynamic model, work by manipulating the dissipation, but that they are otherwise not representative of the subgrid stresses. However, this was in the context of a restricted class of models (eddy viscosity models), and so we ask here whether a more general class of models could be more realistic. In particular, consider the general problem of estimating the subgrid stress term $\mu_i = \partial \tau_{ij}/\partial x_j$ that appears in the LES equations. The only information available is the large-scale field being simulated in the LES. There are presumable many small-scale (subgrid) fields that could occur with the same large scales, which would give rise to different $\boldsymbol{\theta}$. Thus $\boldsymbol{\theta}$ is essentially stochastic, and we should ask how much variation there can be in $\boldsymbol{\theta}$ for a given large-scale field and how good a deterministic estimate of it could possibly be.

The best possible deterministic estimate $\hat{\boldsymbol{\theta}}$ of $\boldsymbol{\theta}$ is sought in the mean-square sense. That is, we seek $\hat{\boldsymbol{\theta}}$ such that the residue $\rho = \langle |\hat{\boldsymbol{\theta}} - \boldsymbol{\theta}|^2 \rangle$ is minimized, where $\langle \cdot \rangle$ is the ensemble average, in this case over all turbulent fields with the same large-scale field. The solution to this minimization problem is well known[16,17] and is given by the conditional average conditioned on the large-scale field $\boldsymbol{u}$:

$$\hat{\boldsymbol{\theta}} = \langle \boldsymbol{\theta} \,|\, \boldsymbol{u} \rangle \tag{10}$$

If one were able to use the conditional average as a model for $\boldsymbol{\theta}$ in an LES, as suggested by Adrian,[18] the instantaneous error in the evolution of the large scales would be minimized. In addition, as was privately pointed out by S. Pope, the multipoint statistics of the simulated large-scale fields would match those of the large scales of the actual turbulence. This feature arises because of the role the conditional average plays in the evolution equation for the probability density function (PDF). In particular, it can be shown[19–21] that, if one has two stochastic evolution equations,

$$\frac{\partial u}{\partial t} = O(u), \qquad \frac{\partial v}{\partial t} = N(v) \tag{11}$$

where N and O are stochastic operators, then if

$$\langle O(u) \,|\, u \rangle = \langle N(u) \,|\, u \rangle \tag{12}$$

the evolution equations for the PDFs $P(u)$ and $P(v)$ will be identical. Thus by choosing the conditional average as our model, we are assured that, in a certain sense, the PDF of the simulated LES field evolves like the PDF of the large-scale turbulence. Because these are the multipoint PDFs, the implication is that the multipoint statistics of the LES and real turbulence also evolve together. Note that there are subtleties of ergodicity associated with the implication of these results for a single LES simulation. A trivial special case of this result is that the conditional average model has the correct dissipation.

Unfortunately, because the conditional average in Eq. (10) is conditioned on the entire large-scale field, these averages cannot be practically computed, but they can be estimated and approximated. Because the conditional average as a model of $\boldsymbol{\theta}$ is essentially an ideal model, one can think of the problem of developing a deterministic LES model as developing an approximation to the conditional average.

A. Estimating the Conditional Average

There is a well-established technique for estimating conditional averages, known as stochastic estimation.[16,17] In this technique one seeks the best approximation to the conditional average (in the mean-square sense), with a given functional dependence on the conditions. For example, in linear estimation one seeks an approximation that is linearly dependent on the condition data. Thus, we estimate our conditional average of the model term as

$$\langle \mu_i \,|\, \boldsymbol{u} \rangle(\boldsymbol{x}) \approx \int_{\mathcal{D}} \Lambda_{ij}(\boldsymbol{x}, \boldsymbol{x}') u_j(\boldsymbol{x}') \, \mathrm{d}\boldsymbol{x}' \tag{13}$$

where the kernel Λ_{ij} can be determined from the integral equation[17,22]

$$\int_{\mathcal{D}} \Lambda_{ij}(\boldsymbol{x}, \boldsymbol{x}') \langle u_j(\boldsymbol{x}') u_k(\boldsymbol{x}'') \rangle \, \mathrm{d}\boldsymbol{x}' = \langle \mu_i(\boldsymbol{x}) u_k(\boldsymbol{x}'') \rangle \tag{14}$$

assuming that the two-point correlations of the velocity with itself and with the model term are known. Similarly, in a quadratic estimate in which one considers one-point quadratic functions of the velocity, the estimator can be found from two-point correlations of quadratic products of the velocity. The linear estimate can also be considered to be the first term in a generalized Taylor expansion; the next term is then based on two-point quadratic functions of the velocity. In this case the estimator is determined from two-, three-, and four-point correlations.

In addition to being the best mean-square estimates of the conditional average, stochastic estimates also minimize the mean-square error of the term being estimated (i.e., the model term). As a consequence, a subset of the results on statistics just discussed applies; for example, using a one-point quadratic estimator as a model, all quadratic and cubic one-point statistics of the large scales (e.g., the Reynolds-stresstensor) of the large-scale field evolve as in the actual turbulent flow. In particular, this includes the dissipation.

B. Predictability of $\boldsymbol{\theta}$

A good measure of the predictability of $\boldsymbol{\theta}$ is just the mean-square error, which can be easily determined once an estimate of the conditional average is available. This is the error between the estimate of the conditional average and the true subgrid stress in a direct numerical simulation (DNS) (as in an a priori test). Thus, the error includes two parts: the error between the conditional average and the true term, which is the minimum error possible, and the error between the stochastic estimate and the conditional average. Experience has shown that stochastic estimates are very good approximations to the conditional average,[23] and so we expect the error to be dominated by the irreducible error between conditional average and the real term. We obtained the estimates and measured the errors using correlation data from a DNS of a forced isotropic turbulence.[21] The simulations were done at $Re_\lambda = 267$ and used 256^3 Fourier spectral modes. Both linear and quadratic estimates were developed for large-scale fields defined using three different Fourier cutoff filters. Spatial averages were used instead of ensemble statistics, but the notation of the latter will be kept here.

As just discussed, the conditional average and its estimates ensure that the dissipation is represented correctly, that is, $\langle \boldsymbol{\tau} \cdot \boldsymbol{\sigma} \rangle = \langle \boldsymbol{u} \cdot \hat{\boldsymbol{\theta}} \rangle = \langle \boldsymbol{u} \cdot \boldsymbol{\theta} \rangle$. The orthogonality of the Fourier functions assures that this is true for each individual Fourier mode, not just for the overall flow as written here. Thus, the component of $\boldsymbol{\theta}$ that is statistically aligned with $\boldsymbol{u}$ is perfectly predicted, and the question is how well can the rest be represented. Define

$$\boldsymbol{\theta}' = \boldsymbol{\theta} - \frac{\langle \boldsymbol{\theta} \boldsymbol{u} \rangle}{\langle \boldsymbol{\theta}^2 \rangle^{\frac{1}{2}} \langle \boldsymbol{u}^2 \rangle^{\frac{1}{2}}} \boldsymbol{\theta} \tag{15}$$

to be the component of $\boldsymbol{\theta}$ that is statistically orthogonal to $\boldsymbol{u}$. The mean square error ρ, normalized by $|\boldsymbol{\theta}|^2$, is shown as a function of wave number in Fig. 4 for the three cutoff filters discussed here. When normalized in this way, the error is (trivially) identically one for linear estimation and no better than 97% for one-point quadratic estimation. The error is so large because the magnitude of the estimates is much smaller than $|\boldsymbol{\theta}|$. When normalized by the magnitude of the whole term $\boldsymbol{\theta}(k)$ (not shown), the error varies from 80 to 98% in the the high wave-number range, where the model term is significant. These values are consistent with the overall 95% of the subgrid stress that is not predicted by Smagorinsky, as discussed in

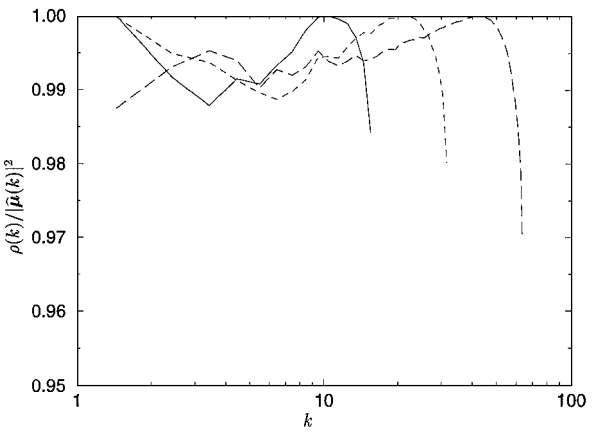

Fig. 4 Error $\rho(k)$ in estimating the subgrid term $\boldsymbol{\theta}$, using a quadratic estimate normalized by the component $\boldsymbol{\theta}'$ of $\boldsymbol{\theta}$ that is statistically orthogonal to $\boldsymbol{u}$. Shown are results for cutoff wave numbers of ——, 16; – – –, 32; and – – –, 64. In this normalization the error of the linear estimate is identically one.

Sec. II.D. The fact that the quadratic estimates have only minutely reduced the error, when they should be significantly better estimates, suggests that the estimates are indeed good approximations to the conditional average, as expected from previous experience.[17]

If the estimates are indeed good approximations to the conditional average as our results suggest, then the orthogonal component $\boldsymbol{\theta}$ is essentially unpredictable given information about just the resolved scales. Furthermore, the predictable component of $\boldsymbol{\theta}$, i.e., that statistically aligned with $\boldsymbol{u}$, is small compared to $\boldsymbol{\theta}$ as a whole, accounting for as much as 20% of the magnitude of the total term for the widest filter and as little as 2% for the narrowest. These measures are related to the correlation coefficient γ estimated in the Appendix, although the normalization is different here ($|\boldsymbol{u}|$ and $|\boldsymbol{\theta}|$ here rather than $|\boldsymbol{\tau}|$ and $|\boldsymbol{\sigma}|$).

Although the substantial unpredictability of the subgrid term in the LES equations seems disappointing, the dissipation by the subgrid term is perfectly predictable and that appears to be enough. These results suggest that, in isotropic turbulence, subgrid models which reproduce the subgrid dissipation are doing as well as is possible. Notice however that it is not just the overall dissipation that can be predicted, but the dissipation at each wave number as well. This has not yet been demonstrated for subgrid models in current use. Furthermore, despite very poor predictions of the actual subgrid stress in a priori tests, there is good reason to expect an LES based on such models to produce reasonable resolved-scale statistics, as has indeed been observed. All of this suggests that setting the constant in Eq. (5) by what amounts to a dissipation matching condition is a sensible approach.

IV. Shear Flows

A. Isotropic Subgrid Stresses

The results in Sec. II.D regarding the lack of correlation between the stresses and the rate of strain tensor raise the question of how models based on an eddy (hyper)viscosity may work in shear flows, where the stresses control the mean flow and are the main quantities to be predicted. The problem is independent of how efficient the model is in adjusting the proportionality coefficient to provide the right dissipation or on the form of the viscosity term. Because, as we note in the Appendix, the correlation between the stress and the strain is directly related to the dissipation $\overline{\boldsymbol{\tau}\cdot\boldsymbol{\sigma}}$ if the correlation level of a particular model is chosen incorrectly and the coefficient in Eq. (3) is adjusted to obtain the right dissipation, the resulting stresses would be wrong, and vice versa.

In models based on an eddy viscosity, the stress and the strain are, by definition, fully correlated at the grid level, and because we have shown that the correlation in real flows is lower, the stresses that the model need to generate the right dissipation will be too low. The isotropic analysis in the Appendix suggests that the correct correlation is of the order of 20–30%, which would imply that either the predicted stresses are too low by a factor of three to five or the strains too high by the same factor. The consequence is that it is impossible to get both the right spectrum and the right stresses from an eddy viscosity.

It is an intriguing possibility that some of the mixed models[7,24] that report improved stress prediction by adding extra terms to the basic eddy viscosity may be doing so by decreasing the strain-stress correlation to more natural levels, especially because similar improvements have been reported in models in which the extra terms are essentially a random force.[25,26]

B. A Priori vs A Posteriori Testing

Before we explore the implications of this apparently discouraging conclusion, some words are needed on the testing of LES models. The obvious test, usually called a posteriori, is to define a figure of merit, such as the mean velocity profile, and to compare the result of the computation with a suitably filtered experimental value. This method has come under attack on the grounds that it characterizes complete codes and does not distinguish numerical from modeling errors so that if the results agree it may be because of compensating errors, whereas if they do not it is usually difficult to isolate the cause.

An a priori method for testing LES models, independently of the numerical factors, was introduced in Ref. 10. Assume that the full flowfield in a given situation is known. It is then possible to compute exactly the grid-filtered field $\{\boldsymbol{u}\}$ and the subgrid stresses. From $\{\boldsymbol{u}\}$, using only information that would be available to the LES code in a real situation one computes the stresses that would be predicted by the proposed model and compares them to the ones derived from the filtered data.

Although this way of testing appears to be an improvement over the earlier one, its results have been disappointing. The subgrid stresses predicted by most models turn out to be only poorly correlated with those measured from the filtered fields[7,10] in spite of which some of those models work well a posteriori. This is often interpreted as meaning that a priori testing is unduly pessimistic, but it is probably closer to the truth to say that the results of standard a priori tests are only weakly related to the performance of subgrid models. Indeed, the results of Sec. III suggest that good performance in a priori tests are neither possible nor required for a good LES model.

In general, all that can be said of the usual a priori testing is that if its results are perfect the model would certainly reproduce exactly the flow, but in the more common case in which the results are poor, nothing can be said about performance in a real situation.

Another difficulty with interpreting a priori tests is that they test how the model represents the effects of subgrid turbulence, but they do it in the wrong flow because the model acts on a different field in the LES simulation than in the test. Whereas the former is the result of the accumulated dynamic effect of the model itself and of the numerics, the latter is just the static application of the model to predict the stresses in a real turbulent flow. Thus a bad model can produce good results because it is acting on a bad flow but is designed to compensate for it. A good example of this is the surprising good performance of the modified dynamic model discussed in Sec. II.B.

But the main reason why a priori testing is restrictive is because many of the desired results of the simulations are large-scale quantities, which reside in flow structures that are being simulated directly and which do not have to be modeled at all. This was clear in the preceding discussion of Figs. 1 and 2, where gross errors in the behavior of the small-scale end of the energy spectrum had only minor effects on the evolution of the total energy. A priori testing of the dissipation generated by the small scales in the modified models would show gross errors, but they only have a small effect on the energy because the desired and the modeled quantities are different. We will next illustrate this point by coming back to the question of the shear stresses.

C. Anisotropic Stresses

Turbulence becomes more isotropic at smaller scales, and it is generally believed that it is essentially isotropic in the inertial range. In shear flows the classical Kolmogorov theory predicts that the spectrum of the normal stresses behaves as $E_{11} \sim \varepsilon^{2/3} k^{-5/3}$, whereas, at least for weak shear S, the cospectrum of the off-diagonal components behaves[27] like $E_{12} \sim S\varepsilon^{1/3} k^{-7/3}$. The consequence is that the subgrid stresses, which are proportional to $\int_k E(k)\,\mathrm{d}k$, decrease like

$$\tau_{12} \sim (kL_s)^{-\frac{4}{3}}, \qquad \tau_{12}/\tau_{11} \sim (kL_s)^{-\frac{2}{3}} \tag{16}$$

where the length $L_s = (\varepsilon/S^3)^{1/2}$ is, for equilibrium flows, proportional to the usual integral scale $L_\varepsilon = q^3/\varepsilon$. It follows that, as the scale of the filter becomes smaller with respect to the integral length, the subgrid shear stress that has to be carried by the model decays even faster than the subgrid energy, and even gross errors in its estimation become negligible for the mean flow. The experimental evidence for this behavior is surveyed in Ref. 28, and a review of some older experiments, seen from the point of view of LES, can be found in Ref. 29.

The latter paper presents a series of LES of a plane channel ($Re_\tau \approx 1000$) at different resolutions, using a standard dynamic-Smagorinsky model averaged over wall-parallel planes, and compares the subgrid shear stress provided by the model with the one derived by filtering a direct simulation at a roughly similar Reynolds number.[30] The LES code uses Fourier expansions in the two wall-parallel directions and B-splines across the channel.[31] Its

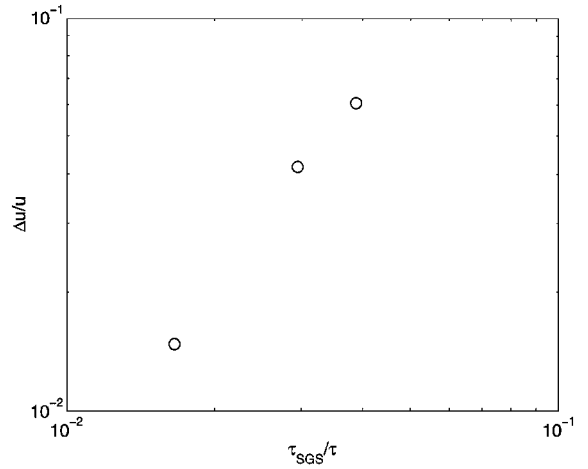

Fig. 5 Rms fractional error of the mean velocity profile as a function of the average fraction of the subgrid stresses carried by the model in the simulations in Fig. 6. Data above $y/h \approx 0.3$.

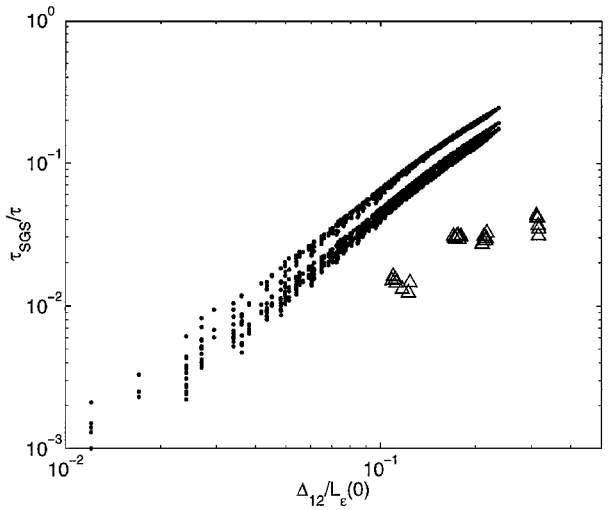

Fig. 6 Fraction of the subgrid shear stress carried by the Smagorinsky model in a channel, as a function of filter size normalized by the integral scale at the centerline: ●, from filtered direct simulation at $Re_\tau \approx 600$ (Ref. 30), and △, from LES at $Re_\tau \approx 1000$ using a Smagorinsky-dynamic model. Only points above $y/h \approx 0.3$ are plotted (adapted from Ref. 29).

multiblock character allows different resolutions in the center of the channel and near the wall, where no good subgrid model is known. The grid below $y^+ \approx 200$ is always the same, and it essentially resolves the flow. The maximum subgrid fraction of τ_{12} in this region is 8% very near the wall but falls quickly below 1%. The grid in the central block is coarsened by factors of 1–3 in the Fourier directions. The wall-normal grid is stretched smoothly across the channel and is identical in all cases. The velocity profile is compared to an independent simulation on a grid refined in all three directions and which agrees with the result of the LES with the finest grid within $\approx 1\%$ (Fig. 5).

The direct simulation is fully resolved. Subgrid stresses are derived by filtering the correlation tensor[32] with a box filter of the same dimensions as the LES grid and are shown as dots in Fig. 6. Gaussian filters with standard deviations equal to the half-widths of the box gave essentially the same results. Because those filters are very anisotropic, an equivalent length is needed to present the results. The geometric mean $(\Delta_1\Delta_2\Delta_3)^{1/3}$, which is often used for Smagorinsky modeling[33] and which can be justified on the grounds of equivalent dissipation, is not a good choice to collapse the stresses. Much better results are obtained with quadratic combinations of the filter widths, which are different for the different stress components and, in some measure, for the different flows. They can be justified as parabolic approximations to the correlation tensor. For τ_{12} in the channel, the best combination was found by Baggett[29] to be

$$\Delta_{12} = \left(\Delta_1^2 + \Delta_2^2 + 4\Delta_3^2\right)^{\frac{1}{2}} \tag{17}$$

which is used in Fig. 6 for a wide range of filter shapes. The collapse is good, and most of the scatter is among different locations in the channel, rather than because of filter anisotropy. The same length is used to reduce the LES results.

Figure 6 clearly shows that the shear stresses predicted by the model are only a fraction of the true ones, and it is interesting that the deficit is close to the factor of five just predicted on isotropic grounds. Note that this is a posteriori testing, in that the effect of the model on its flowfield is being compared with experimental results, but that we are using it to test directly the behavior of the model, i.e., the stresses, rather than its overall effect on the velocity profile. This comparison can never be precise because it is unclear which is the filtering operation implicit in the use of the grid and what to use as an equivalent resolution for the simulation. But the latter can in no case be finer than the grid, and because the fraction of the stresses carried by the resolved scales in an LES increases as the resolution improves, using the width of the grid as an equivalent filter should in any case lead to an overestimation of the predicted stresses. The deficit in Fig. 6 is a genuine underprediction.

This observation is confirmed by Fig. 5, which compares the modeled shear stress fraction, averaged over the central part of the channel, with the resulting fractional error of the predicted velocity profile. The two quantities are roughly proportional and of the same order. The modeling of the stresses is grossly in error, and the only way to get good results is to adjust the resolution so that the subgrid stresses are negligible. Figure 6 shows that this implies, at the 1% error level, filter widths of the order of 5–10% of the integral length. Note that this is, for flows away from walls, an inviscid limit independent of Reynolds number and therefore equally valid for laboratory flows and for industrial applications. It implies $\approx 10^3$ grid points per cubic integral length.

V. Conclusions

We have reviewed the physical basis for the good a posteriori performance of dynamic-Smagorinsky subgrid models in LES and have shown that it appears to be only weakly related to their ability to correctly represent the subgrid physics. We have argued more generally that simulating the correct subgrid physics is not always required to simulate some aspects of the flow and indeed that our ability to model the detailed effects of the subgrid scales may be severely limited by their inherent unpredictability. Thus, it is more important than ever that a fundamental understanding of the physics of the flow, and of the limitations on the models, be an integral part of any decision regarding their applicability and their resolution requirements.

Because of this distinction between physics and modeling, we have suggested that careful a posteriori testing of selected quantities is the best approach to testing and characterizing subgrid models, even from the fundamental point of view. This should in general be done with due consideration of numerical and other effects, but we have tried in this paper to restrict ourselves to the influence of the subgrid model by using high-order or spectral numerical schemes.

We have shown that, apart from their known ability to generate vanishing eddy viscosities in smooth flows, much of the good behavior of dynamic models is because of their robustness to errors in the physics. The reason is that the formula for their eddy viscosity contains a sensor that responds to the accumulation of energy in the high wave numbers of the spectrum before it contaminates the energy containing range. This property is shared by other schemes, and we have suggested that any model with this feedback property, and with roughly correct physics, is likely to represent well the energy of the flow.

By defining an ideal LES model and estimating its properties using DNS data, we showed that there are severe limitations to how well the details of the subgrid term can be modeled. In isotropic turbulence the only quantity that can be exactly predicted is the subgrid dissipation. We also indicated that despite the poor prediction of the subgrid term a model that predicts the predictable part of the

subgrid term will result in an LES that reproduces the large-scale statistics of the real turbulence.

The classical justification of the dynamic model in terms of scale similarity and optimal approximation of the stresses has been examined and found weak. The main problem is that any eddy viscosity model assumes that subgrid stresses are perfectly correlated to the strain, whereas this correlation is poor in real flows. This makes it impossible to predict accurately at the same time the stresses and the energy spectrum. The classical dynamic models are adjusted to predict the latter, and their stresses are low by a substantial factor. We have shown by direct testing in a turbulent channel that this is true even for the mean shear stresses.

We have noted that this poor prediction of the stresses, worrying at first sight for shear flows, can be reduced to a limit on the resolution needed for the application of eddy viscosity models, which should be high enough for most of the stresses to be carried by the resolved scales. The same is true for the flow energy, and in both cases the required grid spacing is of the order of a fraction (≈ 0.1) of the integral flow scale. Although the resulting grids can be large for complex flows, the requirement is independent of the Reynolds number and should therefore be equally applicable to academic and industrial flows. The exception to this optimistic assessment is the flow near walls where the integral scale goes to zero and the grid spacing again becomes dependent on viscosity.[8]

This problem of wall-boundary conditions, although beyond the scope of this review, continues therefore to be the main roadblock to the practical application of LES and will not be solved until a way is found of applying conditions at distances from the wall that do not scale on viscous wall units. The arguments that we have presented suggest that this might be possible without a full consideration of the near-wall flow physics.

The results in this paper lead in fact to the question of whether it may be possible to simulate turbulence without subgrid models, trusting the numerical method to provide the required dissipation. This possibility must however be carefully qualified. Not all numerical dampers are good feedback mechanisms, and most numerical schemes lack the small-scale sensor that we have seen to be a necessary ingredient for robustness. Our discussion of the dynamic model also shows that a certain amount of physics is a desirable property of subgrid models, resulting not only in robustness but in lowest-order accuracy. This is especially true whenever the flow becomes locally laminar because most numerical methods have trouble separating large laminar gradients from turbulent fluctuations. The discussions in this paper, however, suggest that incorporating very detailed physics in subgrid models may only result in moderate savings in computational work and that rather simple approximations might be sufficient in some cases.

Appendix: Isotropic Correlations

Consider equilibrium isotropic turbulence. The dissipation

$$\varepsilon = -\overline{\boldsymbol{\tau} \cdot \{\boldsymbol{\sigma}\}} = -\overline{\boldsymbol{\tau}^* \cdot \{\boldsymbol{\sigma}\}} \tag{A1}$$

is the covariance between the subgrid Reynolds-stress tensor

$$\tau_{ij} = \{u_i u_j\} - \{u_i\}\{u_j\} \tag{A2}$$

and the filtered rate of strain tensor $\boldsymbol{\sigma}$ and should be independent of the filter width. In this Appendix $\{\cdot\}$ represents the grid-filtering operation. The filtered rate of strain is a low-pass-filtered quantity, whereas $\boldsymbol{\tau}$ is a high-pass-filtered one, although with some contributions from low wave numbers that will be discussed next. Assume sharp spectral filtering at wave number k_0. We can define a correlation between the two tensors, equivalent to Eq. (7), as

$$\gamma = \varepsilon \Big/ \left(\overline{|\boldsymbol{\tau}^*|^2}\,\overline{|\boldsymbol{\sigma}|^2}\right)^{\frac{1}{2}} \tag{A3}$$

The norm of the rate-of-strain tensor is best computed directly from its spectrum, which can be written in terms of the energy spectrum using the isotropy relations given in Ref. 34:

$$\overline{|\boldsymbol{\sigma}|^2} = \frac{1}{2}\int_{k\le k_0} k_j^2 \Phi_{ii}\, \mathrm{d}^3k = \int_0^{k_0} E(k) k^2\, \mathrm{d}k \tag{A4}$$

Repeated indices, including squares, imply summation. Estimating the norm of the subgrid stress requires a little more work, although rougher approximations are possible. If we denote by $F(\boldsymbol{x})$ the grid-filtering kernel:

$$\{u\}(\boldsymbol{x}) = \int F(\boldsymbol{y}) u(\boldsymbol{x}-\boldsymbol{y})\, \mathrm{d}\boldsymbol{y} \tag{A5}$$

the subgrid stresses can be interpreted as the result of a double-filtering operation

$$\tau_{ij}(\boldsymbol{x}) = \int H(\boldsymbol{y}, z) u_i(\boldsymbol{x}-\boldsymbol{y}) u_j(\boldsymbol{x}-z)\, \mathrm{d}\boldsymbol{y}\, \mathrm{d}z \tag{A6}$$

where

$$H(\boldsymbol{y}, z) = F(\boldsymbol{y})\delta(\boldsymbol{y}-z) - F(\boldsymbol{y})F(z) \tag{A7}$$

The computation of $\overline{|\boldsymbol{\tau}^*|^2}$ leads to integrals of multipoint combinations of the type $\overline{u_i u_j u_k u_m}$, which can be expressed in terms of two-point correlations using the standard quasi-normal approximation.[34] The resulting integral can then be transformed to Fourier space and written in terms of products of the spectral tensor of the type

$$\int \hat{H}(\boldsymbol{k}, \boldsymbol{q}) \Phi_{ij}(\boldsymbol{k}) \Phi_{mp}(\boldsymbol{q})\, \mathrm{d}\boldsymbol{k}\, \mathrm{d}\boldsymbol{q} \tag{A8}$$

where $\hat{H}(\boldsymbol{k}, \boldsymbol{q})$ is the double Fourier transform of H. For a dealiased sharp cutoff filter in one space dimension, $\hat{H} = 1$ in the strip $|k+q| < k_0$, except where $|k| < k_0$ and $|q| < k_0$, and vanishes otherwise. The vanishing of this filter below $k = k_0$, which is a consequence of subtracting the second term in Eq. (A2), is what makes the subgrid stresses an essentially, although not exactly high-pass filtered quantity, and justifies the estimates made in Eq. (16). In three dimensions the corresponding domain of the six-dimensional integral (A8) extends over the whole Fourier space $\boldsymbol{k}$, but is weighted at each point by an integral over $\boldsymbol{q}$. If $|\boldsymbol{k}| \ge k_0$, the latter extends over the sphere $|\boldsymbol{q}+\boldsymbol{k}| < k_0$, whereas if $|\boldsymbol{k}| < k_0$, it only extends over the spherical crescent bounded on the outside by $|\boldsymbol{q}+\boldsymbol{k}| = k_0$ and on the inside by $|\boldsymbol{q}| = k_0$. The result is that the dominant contribution to the norm of the stresses comes from the neighborhood of $k = k_0$, which can be assumed to be in the inertial range and that the integrals can be evaluated using the inertial form of the energy spectrum

$$E(k) = C_k \varepsilon^{\frac{2}{3}} k^{-\frac{5}{3}}, \qquad C_k \approx 1.5 - 2 \tag{A9}$$

with corrections that are of the order of $(k_0 L_\varepsilon)^{-1/3}$. After substantial, but straightforward, algebraic manipulation,

$$\overline{|\boldsymbol{\tau}^*|^2}^{\frac{1}{2}} \approx 4.6 \varepsilon^{\frac{4}{3}} C_k^2 k_0^{-\frac{4}{3}} \tag{A10}$$

$$\gamma \approx 0.2 - 0.28 \tag{A11}$$

Acknowledgments

Part of this work was carried out at the Center for Turbulence Research and supported by it and by Air Force Office of Scientific Research Grant F49620-97-1-0210. Partial support was also provided by the Spanish CICYT under Contract PB95-0159, by the Instituto Nacional de Técnica Aeronáutica under its combustion program, and by the U.S. National Science Foundation and Air Force Office of Scientific Research under Contract NSF-CTS-9616219. The results in Fig. 6 are due in large part to J. Baggett and A. Kravchenko, and the results in Fig. 4 are due to J. Langford.

References

[1] Rogallo, R. S., and Moin, P., "Numerical Simulations of Turbulent Flows," *Annual Review of Fluid Mechanics*, Vol. 16, 1984, pp. 99–137.

[2] Schumann, U., and Friedrich, R., "On Direct and Large-Eddy Simulation of Turbulence," *Advances in Turbulence*, edited by G. Comte-Bellot and J. Mathieu, Springer–Verlag, Berlin, 1987, pp. 88–104.

[3] Ferziger, J. H., "Large Eddy Simulation," *Simulation and Modelling of Turbulent Flows*, edited by T. B. Gatski, M. Y. Hussaini, and J. L. Lumley, Oxford Univ. Press, New York, 1996, pp. 109–154.

[4]Härtel, C., "Turbulent Flows: Direct Numerical Simulation and Large-Eddy Simulation," *Handbook of Computer Fluid Mechanics*, edited by R. Peyret, Academic, New York, 1996, pp. 284–338.

[5]Lesieur, M., and Metais, O., "New Trends in Large-Eddy Simulations of Turbulence," *Annual Review of Fluid Mechanics*, Vol. 28, 1996, pp. 45–82.

[6]Germano, M., Piomelli, U., Moin, P., and Cabot, W. H., "A Dynamic Subgrid-Scale Eddy Viscosity Model," *Physics of Fluids A*, Vol. 3, No. 7, 1991, pp. 1760–1765.

[7]Bardina, J., Ferziger, J. H., and Reynolds, W. C., "Improved Turbulence Models Based on Large-Eddy Simulation of Homogeneous, Incompressible, Turbulent Flows," Dept. of Mechanical Engineering, TF-19, Stanford Univ., Stanford, CA, May 1983.

[8]Moin, P., and Jiménez, J., "Large-Eddy Simulation of Complex Turbulent Flows," AIAA Paper 93-3099, July 1993.

[9]Moin, P., "Progress in Large-Eddy Simulation of Turbulent Flows," AIAA Paper 97-0749, July 1997.

[10]Clark, R. A., Ferziger, J. H., and Reynolds, W. C., "Evaluation of Subgrid-Scale Models using an Accurately Simulated Turbulent Flow," *Journal of Fluid Mechanics*, Vol. 91, No. 1, 1979, pp. 1–16.

[11]Comte-Bellot, G., and Corrsin, S., "Simple Eulerian Time Correlations of Full and Narrow-Band Velocity Signals in Grid-Generated Isotropic Turbulence," *Journal of Fluid Mechanics*, Vol. 48, No. 2, 1971, pp. 273–337.

[12]Jiménez, J., "On Why Dynamic Subgrid-Scale Models Work," *Annual Research Briefs*, Center for Turbulence Research, Stanford Univ., Stanford, CA, 1995, pp. 25–34.

[13]Lilly, D., "A Proposed Modification of the Germano Subgrid-Scale Closure Method," *Physics of Fluids A*, Vol. 4, No. 4, 1992, pp. 633–635.

[14]Rogallo, R. S., "Numerical Experiments in Homogeneous Turbulence," NASA TM-81315, Sept. 1981.

[15]Piomelli, U., Cabot, W. H., Moin, P., and Lee, S., "Subgrid-Scale Backscatter in Turbulent and Transitional Flows," *Physics of Fluids A*, Vol. 3, No. 3, 1991, pp. 1766–1771.

[16]Adrian, R. J., "On the Role of Conditional Averages in Turbulence Theory," *Turbulence in Liquids*, edited by G. Patterson and J. Zakin, Princeton Science Press, Princeton, NJ, 1977, pp. 323–332.

[17]Adrian, R. J., "Linking Correlations and Structure: Stochastic Estimation and Conditional Averaging," *Zoran P. Zaric Memorial International Seminar on Near-Wall Turbulence*, edited by S. J. Kline and N. H. Afgan, Hemisphere, 1990, pp. 420–436.

[18]Adrian, R. J., "Stochastic Estimation of Subgrid Motions," *Applied Mechanics Review*, Vol. 43, No. 5, 1990, pp. 5214–5218.

[19]Pope, S. B., "PDF Methods for Turbulent Reactive Flows," *Progress in Energy and Combustion Science*, Vol. 11, 1985, pp. 119–192.

[20]Berkooz, G., "An Observation on Probability Density Equations, or, When Do Simulations Reproduce Statistics?," *Nonlinearity*, Vol. 7, 1994, pp. 313–328.

[21]Langford, J., and Moser, R. D., "Optimal LES Formulations for Isotropic Turbulence," *Journal of Fluid Mechanics*, Vol. 398, 1999, pp. 321–346.

[22]Adrian, R. J., "Stochastic Estimation of the Structure of Turbulent Fields," *Eddy Structure Identification*, edited by J. P. Bonnet, Springer–Verlag, New York, 1994, pp. 145–195.

[23]Adrian, R. J., Jones, B. G., Chung, M. K., Hassan, Y., Nithianandan, C. K., and Tung, A. T.-C., "Approximation of Turbulent Conditional Averages by Stochastic Estimation," *Physics of Fluids A*, Vol. 1, No. 1, 1989, pp. 992–998.

[24]Horiuti, K., "A New Dynamic Two-Parameter Mixed Model for Large-Eddy Simulation," *Physics of Fluids*, Vol. 9, No. 9, 1997, pp. 3443–3464.

[25]Chasnov, J. R., "Simulation of the Kolmogorov Inertial Subrange Using an Improved Subgrid Model," *Physics of Fluids A*, Vol. 3, No. 3, 1991, pp. 188–200.

[26]Mason, P. J., and Thomson, D. J., "Stochastic Backscatter in Large-Eddy Simulations of Boundary Layers," *Journal of Fluid Mechanics*, Vol. 242, 1992, pp. 51–78.

[27]Lumley, J. L., "Similarity and Turbulent Energy Spectrum," *Physics of Fluids*, Vol. 10, No. 10, 1967, pp. 855–858.

[28]Saddoughi, S. G., and Veeravali, S. V., "Local Isotropy in Turbulent Boundary Layers at High Reynolds Number," *Journal of Fluid Mechanics*, Vol. 268, 1994, pp. 333–372.

[29]Baggett, J. S., Jiménez, J., and Kravchenko, A. G., "Resolution Requirements in Large-Eddy Simulations of Shear Flows," *Annual Research Briefs*, Center for Turbulence Research, Stanford Univ., Stanford, CA, 1997, pp. 51–66.

[30]Moser, R. D., Kim, J., and Mansour, N. N., "Direct Numerical Simulation of Turbulent Channel Flow up to $Re_\tau = 590$," *Physics of Fluids*, Vol. 11, No. 4, 1999, pp. 943–945 (data from case PCH10 of AR-345, AGARD, 1998).

[31]Kravchenko, A. G., Moin, P., and Moser, R., "Zonal Embedded Grids for Numerical Simulations of Wall-Bounded Turbulent Flows," *Journal of Computational Physics*, Vol. 127, No. 2, 1996, pp. 412–423.

[32]Jiménez, J., and Moser, R. D., "Data Filtering and File Formats," *A Selection of Test Cases for the Validation of Large-Eddy Simulations of Turbulent Flows*, AR-345, AGARD, 1998, pp. 5–8.

[33]Deardorff, W., "A Numerical Study of Three-Dimensional Turbulent Channel Flow at Large Reynolds Numbers," *Journal of Fluid Mechanics*, Vol. 41, No. 2, 1970, pp. 453–480.

[34]Batchelor, G. K., *The Theory of Homogeneous Turbulence*, Cambridge Univ. Press, Cambridge, England, U.K., 1953, pp. 49 and 179.

C. G. Speziale
Associate Editor